Dual Regime Spray Deposition Based Laser Direct Writing of Metal Patterns on Polymer Substrates

Semih Akin
School of Mechanical Engineering,
Purdue University,
West Lafayette, IN 47907
e-mail: sakin@purdue.edu

Ted Gabor
School of Mechanical Engineering,
Purdue University,
West Lafayette, IN 47907
e-mail: tgabor@purdue.edu

Seunghwan Jo
School of Mechanical Engineering,
Purdue University,
West Lafayette, IN 47907
e-mail: jo30@purdue.edu

Hangeun Joe
School of Mechanical Engineering,
Purdue University,
West Lafayette, IN 47907
e-mail: hjoe@purdue.edu

Jung-Ting Tsai
School of Materials Engineering,
Purdue University,
West Lafayette, IN 47907
e-mail: tsai92@purdue.edu

Yeonsoo Park
School of Mechanical Engineering,
Purdue University,
West Lafayette, IN 47907
e-mail: park1120@purdue.edu

Chi Hwan Lee
School of Mechanical Engineering,
Purdue University,
West Lafayette, IN 47907
e-mail: lee2270@purdue.edu

Min Soo Park
Department of Mechanical System Design Engineering,
SeoulTech,
Seoul 01811, South Korea
e-mail: lee2270@purdue.edu

Martin Byung-Guk Jun[1]
School of Mechanical Engineering,
Purdue University,
West Lafayette, IN 47907
e-mail: mbgjun@purdue.edu

In recent years, the metallization of polymers has been intensely studied as it takes advantage of both plastics and metals. Laser direct writing (LDW) is one of the most widely used technologies to obtain metal patterns on polymer substrates. In LDW technology, different methods including injection-molding, drop-casting, dip coating, and spin coating are utilized for surface preparation of polymer materials prior to the laser activation process. In this study, an atomization based dual regime spray coating system is introduced as a novel method to prepare the surface of the materials for LDW of metal patterns. Copper micropatterns on the polymer surface were achieved with a minimum feature size of 30 μm, having a strong adhesion and excellent conductivity. The results show that the dual regime spray deposition system can be potentially used to obtain uniform thin film coating with relatively less material consumption on the substrates for surface preparation of laser direct metallization of polymers. [DOI: 10.1115/1.4046282]

Keywords: laser direct writing, silver nanowires, polymer materials, selective metallization, spray deposition

1 Introduction

Over the last few decades, the metallization of polymers has been intensely studied due to its potential applications in automation, robotics, sensors, conducting wires, photovoltaic cells, and anti-electrostatic coating [1,2]. Additionally, increasing demand for small, lightweight, and high-speed portable and wearable electronics devices has created a significant need for a new technology, which enables an efficient fabrication process for the metallization of polymers and overcomes the environmental problems [1,3,4]. Thereby, the laser direct writing (LDW) and selective metallization have drawn a significant attention due to its wide applications including flexible electronics, light-emitting displays, medical equipment, automotive, microelectronics, bioelectronics, and so on [5–7].

As a prominent technique, laser direct writing technology utilizes lasers that have an ultrashort pulse width and extremely high peak intensity. This property provides unique advantages in material processing, which cannot be achieved by traditional methods. The major advantages that laser direct metallization technology has over other methods include design flexibility, short fabrication cycle, accuracy, ease of integration, mask-free processing, and feasibility for large-scale manufacturing [6]. This technology also allows the fabrication of ultrafine structures, which have less than 100 μm widths and gaps [8].

Over the years, many different direct writing techniques have been developed to meet the demand for metal patterns on polymer materials. The main difference among these techniques is the way polymers are prepared for the laser activation process. One of the material preparation methods for LDW is through injection-molding [9–11]. In this method, the additives (generally metal oxide or organic metal complex) are placed inside the polymer matrix using injection molding. However, only the metal seeds that are close enough to polymer surface are activated by laser irradiation. In other words, the rest of these seeds are not used in that process. Furthermore, injection molding has its own drawbacks: it is not a flexible process, it is not efficient for material consumption, it is limited to thin-walled parts, it has high tooling and equipment cost, and it has a long lead time. Another method used to prepare the surface is drop-casting [12–14]. Although drop-casting is a very simple method and not waste a lot of material, this method has significant drawbacks such as poor thickness control, poor uniformity, limitations in large area coating, and so on. Dip coating is another method used to obtain thin film on polymer materials [15,16]. Even though dip coating is easy, fast, cost-effective and suitable for large surfaces, it also has some significant shortcomings such as requiring a large amount of coating liquid, having a low deposition rate, and difficulty of controlling the coating thickness [17].

[1]Corresponding author.

Contributed by the Manufacturing Engineering Division of ASME for publication in the Journal of Micro- and Nano-Manufacturing. Manuscript received November 4, 2019; final manuscript received January 20, 2020; published online March 27, 2020. Assoc. Editor: Lawrence Kulinsky.

One of the other surface preparation methods is spin-coating [18–20]. Although thin films can be obtained quickly, simply, and uniformly by the spin-coating method, this technique also has some important limitations, which are waste of the solution, limitation for only 2D surfaces.

In this study, an atomization based dual regime spray coating system is developed as an innovative method for surface preparation of the materials for LDW of polymers. In the described design, the silver nanowires (AgNWs) solution is first atomized by the droplet generator and the droplets are then carried to the substrate through the central high-speed airflow. Therefore, the proposed system attempts to overcome the limitations of currently used techniques. The experimental results show that the designed spray deposition system could be successfully used for surface preparation of the polymers for direct metallization.

2 Design

In the spraying process, the type of droplet impingement has a significant effect on the quality of the deposition. In general, there are four impingement regimes identified in the droplet–substrate interaction phenomenon [21]. As shown in Fig. 1, the first regime is the stick regime, which occurs when an impinging droplet adheres to the substrate in nearly a spherical form. This often happens when the impact energy is extremely low. The second is the rebounding regime where the impinging droplet bounces off the substrate. The third regime, spreading, is where wetting occurs. Finally, the fourth regime is where splashing or further atomization occurs, and the droplet breaks into many secondary droplets.

The parameters that influence the impingement dynamics of the atomization process are the diameter (d_0) and velocity (w_0) of the incident droplet, the liquid dynamic viscosity (μ), density (ρ), and surface tension (σ) [22]. The conditions of the receiving surface such as the film thickness (h) for wet surfaces also play a major role in controlling the outcome of a droplet–surface collision. The regime transition criteria are determined based on the Reynolds number, the Weber number, Ohnesorge number, and the film thickness number of the incident droplet [22]. The Reynolds number, the Weber number, Ohnesorge number, and the film thickness number are defined as

$$\mathrm{Re} = \frac{\rho w_0 d_0}{\mu} \tag{1}$$

$$\mathrm{We} = \frac{\rho w_0^2 d_0}{\sigma} \tag{2}$$

$$\mathrm{Oh} = \frac{\mu}{\sqrt{d_0 \sigma \rho}} \tag{3}$$

$$h_{\mathrm{nd}} = \frac{h}{d_0} \tag{4}$$

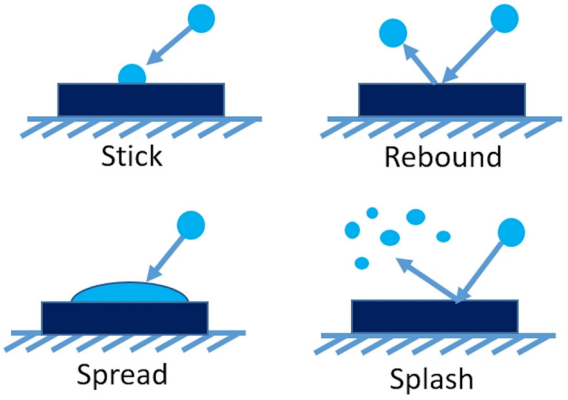

Fig. 1 Modes of the droplet–surface interaction

Table 1 Criteria of impingement regimes for dry walls

Regime	Criterion	References
Stick	$\mathrm{We} < 5$	[23]
Rebound	$5 < \mathrm{We} < 10$	[23,24]
Spread	$10 < \mathrm{We} < 18^2 d_d \left(\frac{\rho}{\sigma}\right)^{1/2} v^{1/4} f^{3/4}$	[25]
Splash	$18^2 d_d \left(\frac{\rho}{\sigma}\right)^{1/2} v^{1/4} f^{3/4} < \mathrm{We}$	[25,26]

where ρ is the liquid density, w_0 is the droplet normal to the impact surface, d_0 is the droplet diameter, μ is the liquid dynamic viscosity, h is the film thickness, and h_{nd} is the nondimensional film thickness number. The criteria of impingement regimes for dry walls are given in Table 1. In the equation given for the spread regime criterion, v is kinematic viscosity and f is the frequency of impinging drops. f is also known as the splashing threshold for the multidrop impact with a thin liquid film [25].

Establishing a rebound regime within the deposition system before the droplets leave the nozzle is important for a coating system consists of a spray generation unit and nozzle. Accordingly, it helps to prevent the condensation of liquid on tube and nozzle walls and building up of material on the internal surfaces [27]. Therefore, the Weber number should be selected as $5 < \mathrm{We} < 10$ to satisfy the rebound regime for the traveling droplets to the nozzle. On the other hand, droplets should spread on the substrate to provide optimum distribution and adhesion of deposited material [27]. Therefore, a nondimensionless number, K_m, was employed by Mundo et al. [26] to provide a guideline for the splashing regime. To prevent splashing, the criterion should satisfy $K_m < K_{\mathrm{mc}}$ where $K_{\mathrm{mc}} = 57.7$ and the formula for the K_{m} is defined as

$$K_m = (\mathrm{Oh}^{-2/5}\mathrm{We})^{5/8} \tag{5}$$

A dual-regime nozzle design is a very good candidate to ensure the rebound condition on the internal surfaces as well as preventing splashing on the substrate. The dual-regime spray deposition system can efficiently deposit droplets on the substrate minimal material waste. Furthermore, decoupling the atomizer and the nozzle provides better control of spray velocity and deposition [27]. Hence, the system given in Fig. 2 was employed to overcome the limitations of currently available techniques, which are used for surface preparation for LDW of polymers.

In this system, the AgNWs solution was atomized by the pneumatic atomizer. Then, the low-velocity carrier gas takes the droplets to the deposition nozzle through a T-connection. At the nozzle exit, the particles are accelerated and focused through the high-speed velocity air applied in the center of the nozzle. Furthermore, a flow-conditioning unit (FCU) was added to the system in order to prevent condensation and provide uniform droplet size

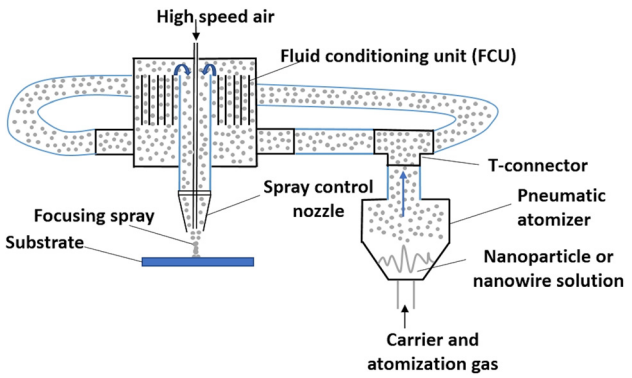

Fig. 2 Schematic of the dual regime spray system

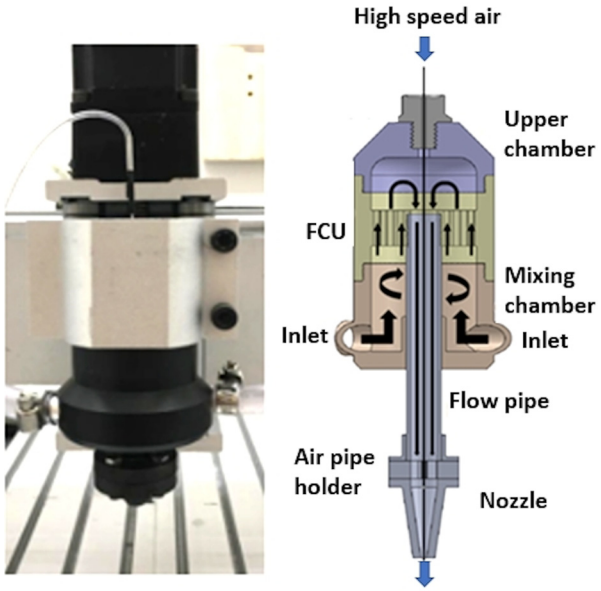

Fig. 3 The nozzle mounted on a computer numerical control router (left), three-dimensional section model of the nozzle (right)

and symmetry of the particle stream. Larger particles collide with the wall of the FCU due to the cyclone effect, they condense, and drained out of the FCU [27]. The three-dimensional computer-aided design model of the nozzle and the fabricated nozzle are shown in Fig. 3.

3 Experimental Section

3.1 Materials. The Kapton polyimide-poly(4,4′-diphenylene pyromellitime, PI) film, whose thickness is 127 μm (0.005″), the temperature range is −450 to 750 °F, and tensile stress is 16,500 psi, was supplied by the DuPont Co., Inc., as a polymer substrate. AgNWs having several hundred nanometer length were home-made synthesized using the polyol method [28].

3.2 Atomization-Based Dual Regime Spray Coating. The AgNWs were deposited on the Kapton polyimide film using the described spray deposition system. The spray system was mounted in a three-axis computer numerical control router to control the motion of the nozzle. It was observed that three parameters, which are atomization and central gas pressure, nozzle transverse speed, and nozzle stand-off distance, have a significant effect on final deposition quality and subsequent metallization processes. Atomization pressure determines the amount of the deposited AgNWs seeds on the surface. The central gas affects the uniformity of the coating focusing the AgNWs droplets onto the substrate. Moreover, transverse nozzle speed and nozzle stand-off distance also have an important effect on the uniformity of the coating. Therefore, proper selection of these parameters is needed to uniformly deposit enough AgNWs seeds on the substrate for direct metallization. Thereby, when these parameters are carefully considered, the atomization pressure and high-speed air stagnation pressure were adjusted to 3 and 31 psi, respectively. The nozzle standoff distance and nozzle transverse speed were fixed to 5 mm and 50 mm/min, respectively. Hence, the atomization flowrate of the AgNWs solution was measured as 0.00272 ml/s, which corresponds to relatively less amount of AgNWs solution.

3.3 Selective Laser Irradiation. Ultrafast lasers have been widely used to irradiate the AgNWs films coated on the polymer substrates [29,30]. Herein, the surface selective activation (irradiation) was performed via the ultrafast laser machining system

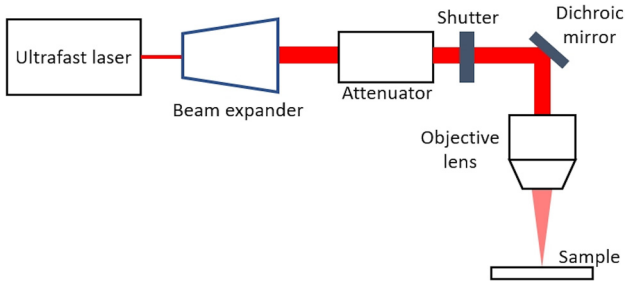

Fig. 4 The schematic diagram of the laser irradiation process

(04-1000, CARBIDE, Light Conversion, Lithuania), which can provide 1030 nm center wavelength, 229 fs–10 ps pulses with a maximum power of 4 W, and repetition rate of 1 MHz. The laser parameters were selected based upon two criteria: (1) rapid irradiation of the polymer and AgNWs film to prevent the oxidation of AgNWs, (2) provide enough porosity on the polymer surface to increase anchoring effect for the plating process. Therefore, considering this criterion the coated AgNWs film was irradiated in air atmosphere with the laser pulse width of 10 ps, the laser frequency of 10 kHz, and the laser pulse energy of 1.1 μJ. The laser scanning speed was set to 4 mm/s. The laser beam was focused onto the polymer film by a 20× microscope objective lens (Mitutoyo, 042 NA), and the fluence of the focused beam was 14.7 J/cm^2. The sample was placed perpendicular to the laser beam and it was moved in x–y direction by computer-controlled Hybrid Hexapod stage. The schematic representation of the laser selective irradiation process is given in Fig. 4. After selective laser irradiation, the samples were cleaned with de-ionized (DI) water in an ultrasonic bath for 5 min at ambient temperature to remove the residual AgNWs.

3.4 Electroless Copper Plating. In this study, a homemade electroless copper plating (ECP) solution was used, which contains 18 g/L of copper sulfate pentahydrate ($CuSO_4{\cdot}5H_2O$) as a source of Cu^{2+} ions, 48 g/L of ethylene diamine tetra-acetic acid as the chelating agent, 0.05 g/L of potassium ferrocyanide ($K_4Fe(CN)_6$) as the stabilizing agent, 18 ml/L of hydrochloric acid (1 N HCl) and 15 ml/L of formaldehyde (HCHO) as the reducing agent in DI water. In the process of electroless plating, the substrate was immersed in the solution for 8 h at room temperature and pH value of the ECP solution was adjusted to 12.0 via NaOH. After the plating, the samples were rinsed with DI water in an ultrasonic bath for 5 min at room temperature. The schematic illustration of the fabrication process is shown in Fig. 5.

4 Results and Discussions

4.1 Scanning Electron Microscopy and Energy-Dispersive X-Ray Characterization. Scanning electron microscopy (SEM) (Hitachi S-4800) was conducted to investigate the morphology of the deposited AgNWs and the fabricated copper patterns.

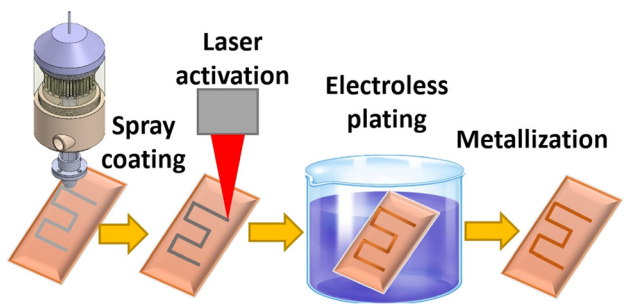

Fig. 5 Schematic illustration of the fabrication process

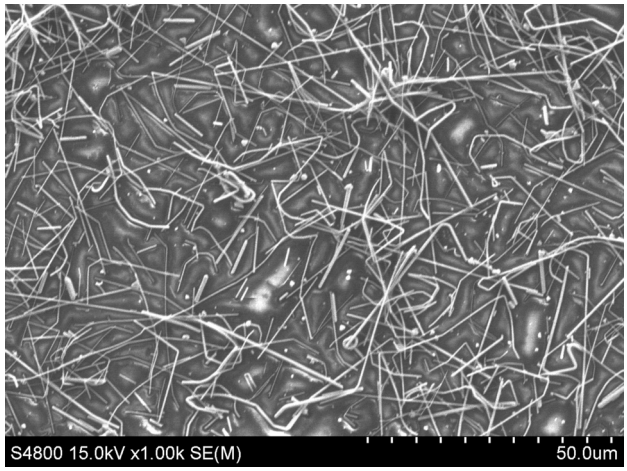

Fig. 6 SEM image of the deposited AgNWs onto PI sample

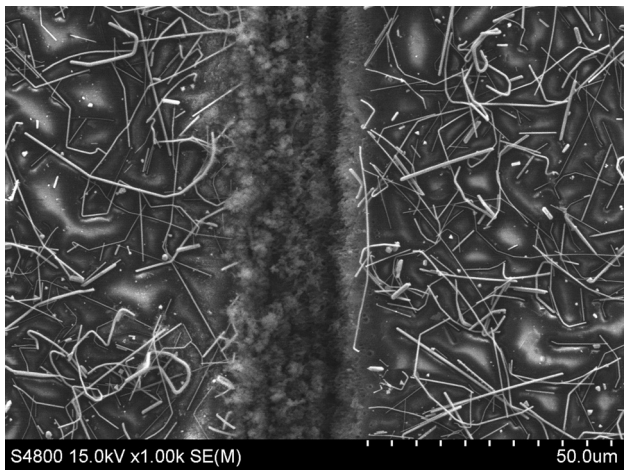

Fig. 7 SEM image of the surface morphology after laser activation

As can be seen in Fig. 6, the AgNWs were successfully deposited onto the surface of the PI film using the dual regime spray deposition system. The surface morphology after the laser irradiation is given in Fig. 7. As shown in Fig. 7, the laser-irradiated area has clear boundaries comparing to the unirradiated area.

After ultrasonic cleaning, the specimen was immersed in the ECP solution for 8 h. Through this process, as can be seen from Fig. 8(*a*), the copper formation was successfully achieved on only selectively laser-irradiated regions. Energy-dispersive X-ray (EDX) analysis was also performed by the (Quanta FEG 650) scanning electron microscope equipped with X-ray (EDX) detector for the plated samples. Given the EDX analysis results as shown in Fig. 8(*b*), the main elements on the PI surface are carbon, oxygen, and copper, having the wt % of 91.15% Cu, 7.07% C, and 1.78% O, respectively.

Using the described method, several circuit patterns were also fabricated on the PI samples as illustrated in Fig. 9. Optical microscope images of the fabricated circuits were taken by an optical microscope (AmScope ME300TZA-SL). As can be seen from Fig. 9, even the sharp edges of the patterns were successfully plated. Moreover, the lines that have less than 30 μm gaps were selectively plated, having very fine resolution without any intersection problem.

4.2 Surface Roughness Measurement. Surface roughness analysis of the fabricated copper patterns was conducted using the

(*a*)

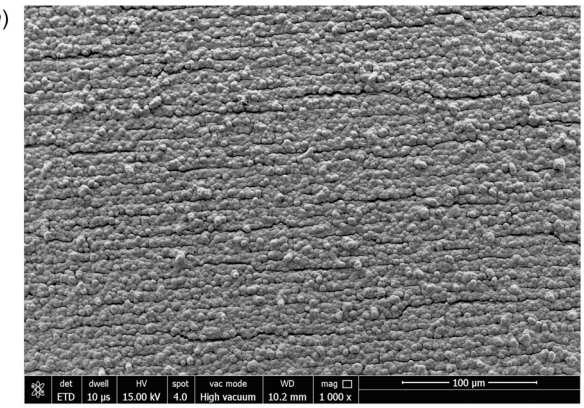

(*b*)

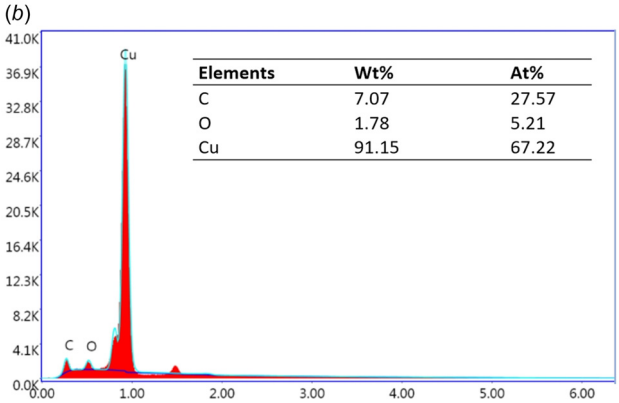

Elements	Wt%	At%
C	7.07	27.57
O	1.78	5.21
Cu	91.15	67.22

Fig. 8 (*a*) SEM image of fabricated copper on the PI sample and (*b*) EDX analysis of the PI surface after 8 h ECP

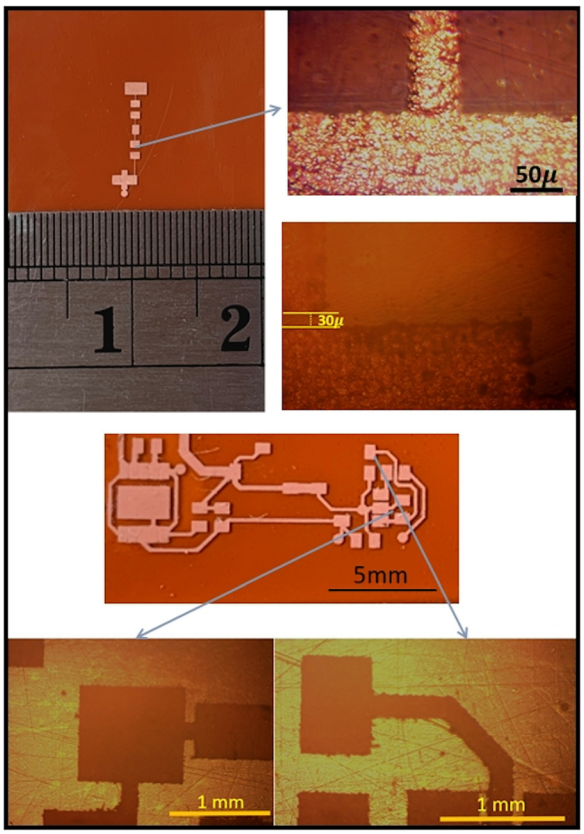

Fig. 9 Fabricated copper patterns on the PI film

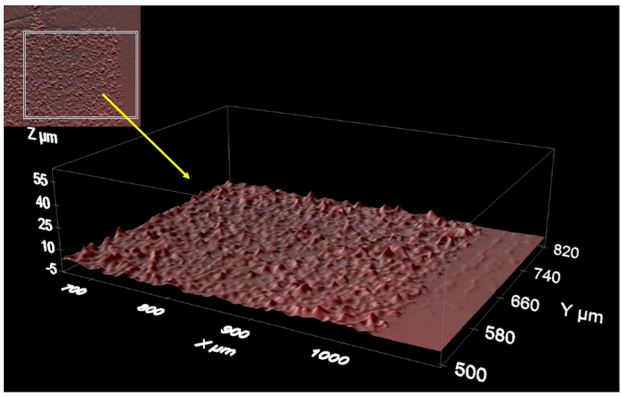

Fig. 10 Isometric view of the surface roughness of the fabricated copper

confocal laser scanning microscope (Leica Microsystems). According to the surface roughness analysis results shown in Fig. 10, it could be said that the surface is relatively rough compared to the original polymer surface. This can be also seen from the SEM image of the surface after the 8 h ECP process as shown in Fig. 8(*a*).

One reason for this situation could be the copper formation during the ECP process since coppers are not formed uniformly, resulting in a relatively rough surface. Additionally, surface roughness analyses for both x and y directions are given in Figs. 11(*a*) and 11(*b*). According to Figs. 11(*a*) and 11(*b*), the height deviation in both x and y direction is more than 7 μm in some regions of the fabricated patterns. This situation could be considered more carefully, where the surface roughness is an important criterion for the application.

4.3 Electrical Performance Measurement. The electrical properties of the obtained copper patterns were analyzed by the four-point probe system (Jandel, RM3-AR) with a constant current of 10 mA at room temperature to remove any contact resistance error from the measurements. The average sheet resistance was determined from five consecutive regions along with the fabricated copper patterns. From these tests, the mean sheet resistance of the fabricated copper pattern was measured as 6 mΩ/sq. In addition, the sheet resistivity formula given in Eq. (5) was used to calculate the resistivity value of the fabricated copper pattern where 4.532 is a correction factor regarding the shape of the cell, R_s is the sheet resistance, ρ is the resistivity, and t is the sheet thickness [31]

$$\rho = 4.532 \times R_s \times t \tag{6}$$

The sheet thickness was obtained from cross section SEM image analysis shown in Fig. 12. Thus, the resistivity of the fabricated copper pattern was calculated as 8.973×10^{-7} Ω m, indicating a high conductivity.

4.4 Adhesion Test. The metal/polymer adhesion performance is an important parameter in terms of the application aspect. Given that, we conducted a standard scotch-tape test (ASTM D3359-02 standard) to evaluate the adhesion property of the copper layer on the polymer substrate. After the tape was peeled off, it was observed that the edges of the cuts are very smooth,

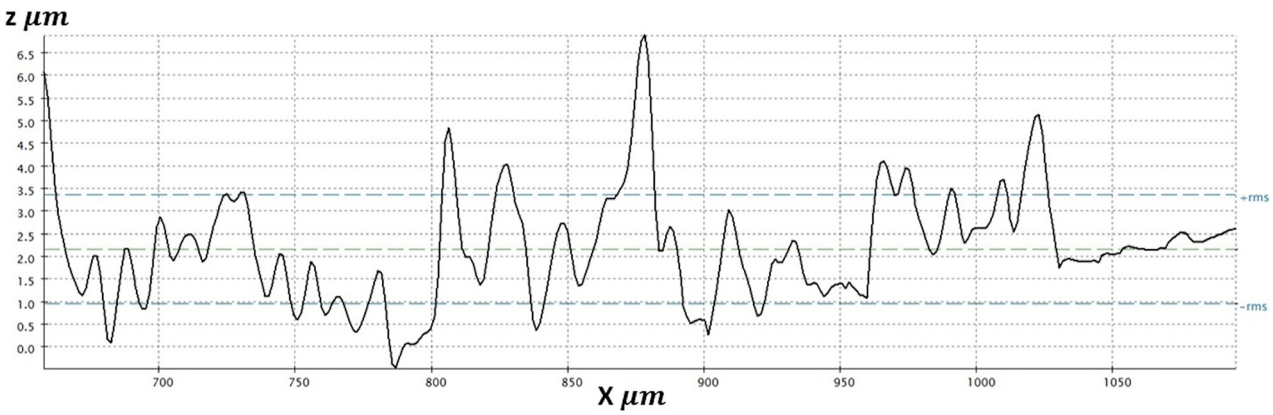

(*a*)

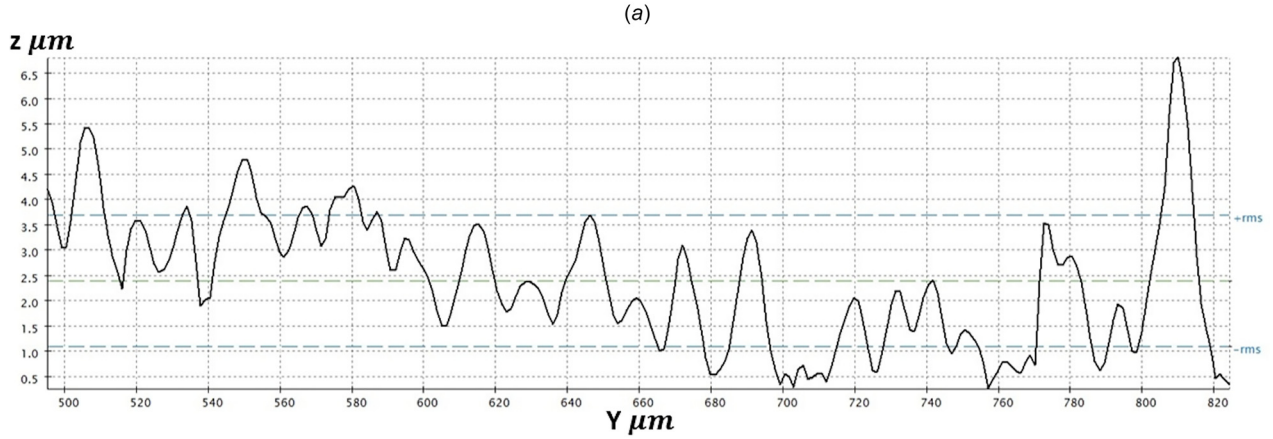

(*b*)

Fig. 11 (*a*) Surface roughness in *x*-direction and (*b*) surface roughness in *y*-direction

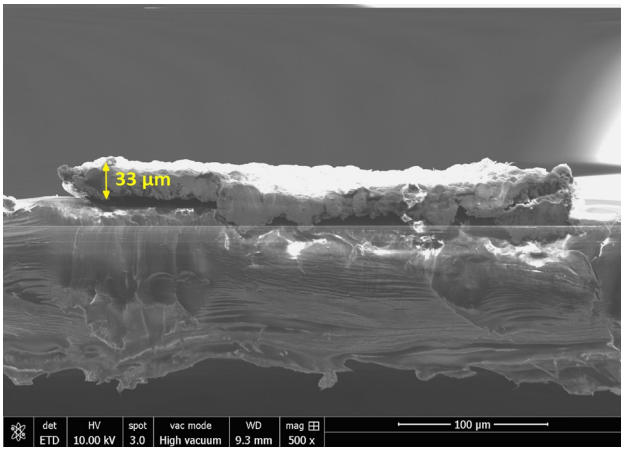

Fig. 12 SEM image of the fabricated copper pattern on PI film

showing a very good adhesion, having the scale of 4 and 5 with respect to ASTM D3359-02 standard. These results meet the requirements for industrial applications.

5 Conclusions

In this article, an atomization-based dual regime spray deposition system was presented as a novel method for surface preparation for laser direct metallization of polymers. AgNWs were successfully deposited on the PI film requiring a relatively small amount of the AgNWs solution (0.00272 ml/s). Moreover, the described system does not require masking owing to the presence of three-axis motion control. This also reduces the amount of coating material consumption. The deposition head also has two inlet sections, enabling the mixing of two different coating solutions. Therefore, the spray system could be easily used where the deposition control of two different solution mixture is needed.

Furthermore, to show the success of the spray deposition method for the laser direct metallization, copper patterns were successfully fabricated on the PI film followed by selective laser irradiation and ECP processes. SEM images indicated that microroughness morphology obtained at the laser-irradiated area, which provides additional anchoring areas for the subsequent ECP process. The EDX analysis showed that the copper content on the fabricated patterns is 91.15 wt %, and the main elements on the polymer surface are copper, oxygen, and carbon. Based on electrical conductivity measurements, the fabricated copper patterns exhibited excellent conductivity (8.973×10^{-7} Ω m), which is comparable to bulk copper resistivity. Moreover, the obtained copper layers have a very good adhesion property according to the scotch-tape test results. Given the surface roughness analysis, however, the surface of the obtained copper layers is relatively rough in both x and y direction due to nonuniform copper formation during the ECP process.

Overall, the main advantages of the described spray deposition system are greatly reduced material consumption, spray deposition control, elimination of masking, increased process flexibility, and suitability for multi-automation and large-scale manufacturing. Furthermore, the described deposition system could be easily integrated with a multi-axis robotic arm for spraying complex curvature parts. This work may find application in a field of area where the material consumption, deposition control, masking, and/or flexibility are an issue and conductive metal pattern with higher resolution is required on the polymer substrates. It is also noteworthy to mention that the given spray deposition system could be easily integrated into conventional LDW technology.

Funding Data

- Republic of Turkey Ministry of National Education.
- The Office of Overseas Scholarship Programs and Technology Innovation Program (10053248) funded by the Ministry of Trade, Industry & Energy (MOTIE), Korea (Funder ID: 10.13039/501100003052).

References

[1] Żenkiewicz, M., Moraczewski, K., Rytlewski, P., Stepczyńska, M., and Jagodziński, B., 2015, "Electroless Metallization of Polymers," Arch. Mater. Sci. Eng., **74**(2), pp. 67–76.
[2] Pandey, R., Jian, N., Inberg, A., Palmer, R. E., and Shacham-Diamand, Y., 2017, "Copper Metallization of Gold Nanostructure Activated Polypyrrole by Electroless Deposition," Electrochim. Acta, **246**, pp. 1210–1216.
[3] Watanabe, A., and Cai, J., 2017, "Selective Metallization Based on Laser Direct Writing and Additive Metallization Process," Proc. SPIE **10092**, p. 100920Z.
[4] Sugioka, K., Gu, B., and Holmes, A., 2007, "The State of the Art and Future Prospects for Laser Direct-Write for Industrial and Commercial Applications," MRS Bull., **32**(1), pp. 47–54.
[5] Zhang, J., Zhou, T., Wen, L., Zhao, J., and Zhang, A., 2016, "A Simple Way to Achieve Legible and Local Controllable Patterning for Polymers Based on a Near-Infrared Pulsed Laser," ACS Appl. Mater. Interfaces, **8**(3), pp. 1977–1983.
[6] Zhang, J., Zhou, T., Wen, L., and Zhang, A., 2016, "Fabricating Metallic Circuit Patterns on Polymer Substrates Through Laser and Selective Metallization," ACS Appl. Mater. Interfaces, **8**(49), pp. 33999–34007.
[7] Zhang, J., Zhou, T., and Wen, L., 2017, "Selective Metallization Induced by Laser Activation: Fabricating Metallized Patterns on Polymer Via Metal Oxide Composite," ACS Appl. Mater. Interfaces, **9**(10), pp. 8996–9005.
[8] Huske, M., Kickelhain, J., Muller, J., and Eber, G., 2001, "Laser Supported Activation and Additive Metallization of Thermoplastics for 3D-MIDs," Proceedings of the Third LANE, Erlangen, Germany, Aug. 28–31.
[9] Yang, J.-u., Cho, J. H., and Yoo, M. J., 2017, "Selective Metallization on Copper Aluminate Composite Via Laser Direct Structuring Technology," Composites, Part B, **110**, pp. 361–367.
[10] Amend, P., Pscherer, C., Rechtenwald, T., Frick, T., and Schmidt, M., 2010, "A Fast and Flexible Method for Manufacturing 3D Molded Interconnect Devices by the Use of a Rapid Prototyping Technology," Phys. Procedia, **5**, pp. 561–572.
[11] Islam, A., Hansen, H. N., Tang, P. T., and Sun, J., 2009, "Process Chains for the Manufacturing of Molded Interconnect Devices," Int. J. Adv. Manuf. Technol., **42**(9–10), pp. 831–841.
[12] Cai, J., Lv, C., and Watanabe, A., 2018, "Laser Direct Writing and Selective Metallization of Metallic Circuits for Integrated Wireless Devices," ACS Appl. Mater. Interfaces, **10**(1), pp. 915–924.
[13] Cai, J., Lv, C., Aoyagi, E., Ogawa, S., and Watanabe, A., 2018, "Laser Direct Writing of a High-Performance All-Graphene Humidity Sensor Working in a Novel Sensing Mode for Portable Electronics," ACS Appl. Mater. Interfaces, **10**(28), pp. 23987–23996.
[14] Mizeikis, V., Chatterjee, S., and Faniayeu, I., 2018, "Direct Laser Writing of Electromagnetic Metasurfaces for Infra-Red Frequency Range," Proc. SPIE **10544**, p. 105440X.
[15] Xu, J., Liao, Y., Zeng, H., Zhou, Z., Sun, H., Song, J., Wang, X., Cheng, Y., Xu, Z., Sugioka, K., and Midorikawa, K., 2007, "Selective Metallization on Insulator Surfaces With Femtosecond Laser Pulses," Opt. Express, **15**(20), pp. 12743–12748.
[16] Liu, Z., Fu, H., Hunegnaw, S., Wang, J., Merschky, M., Magaya, T., Mieno, A., Shorey, A., Kuramochi, S., Akazawa, M., and Yun, H., 2016, "Electroless and Electrolytic Copper Plating of Glass Interposer Combined With Metal Oxide Adhesion Layer for Manufacturing 3D RF Devices," IEEE 66th Electronic Components and Technology Conference (ECTC), Las Vegas, NV, May 31–June 3, pp. 62–67.
[17] Hussmann, E. K., 1983, "Dip Coatings: Characteristics, Properties, Applications," Proc. SPIE **0381**, pp. 152–159.
[18] Watanabe, A., Cai, J., Ogawa, S., Aoyagi, E., and Ito, S., 2018, "Laser Direct Writing Using Nanomaterials and Device Applications Towards IoT Technology," Proc. SPIE **10813**, p. 108130K.
[19] Huang, K. M., Tsai, S. C., Lee, Y. K., Yuan, C. K., Chang, Y. C., Chiu, H. L., Chung, T. T., and Liao, Y. C., 2017, "Selective Metallic Coating of 3D-Printed Microstructures on Flexible Substrates," RSC Adv., **7**(81), pp. 51663–51669.
[20] Dai, X., Wu, J., Qian, Z., Wang, H., Jian, J., Cao, Y., Rummeli, M. H., Yi, Q., Liu, H., and Zou, G., 2016, "Ultra-Smooth Glassy Graphene Thin Films for Flexible Transparent Circuits," Sci. Adv., **2**(11), p. e1601574.
[21] Stanton, D. W., and Rutland, C. J., 1998, "Multi-Dimensional Modeling of Thin Liquid Films and Spray-Wall Interactions Resulting From Impinging Sprays," Int. J. Heat Mass Transfer, **41**(20), pp. 3037–3054.
[22] Trujillo, M. F., Mathews, W. S., Lee, C. F., and Peters, J. E., 2000, "Modelling and Experiment of Impingement and Atomization of a Liquid Spray on a Wall," Int. J. Engine Res., **1**(1), pp. 87–105.
[23] Yarin, A. L., and Weiss, D. A., 1995, "Impact of Drops on Solid Surfaces: Self-Similar Capillary Waves, and Splashing as a New Type of Kinematic Discontinuity," J. Fluid Mech., **283**, pp. 141–173.

[24] Rodriguez, F., and Mesler, R., 1985, "Some Drops Don't Splash," J. Colloid Interface Sci., **106**(2), pp. 347–352.
[25] Stow, C. D., and Hadfield, M. G., 1981, "An Experimental Investigation of Fluid Flow Resulting From the Impact of a Water Drop With an Unyielding Dry Surface," Proc. R. Soc. London, Ser. A., **373**(1755), pp. 419–441.
[26] Mundo, C., Sommerfeld, M., and Tropea, C., 1995, "Droplet-Wall Collisions: Experimental Studies of the Deformation and Breakup Process," Int. J. Multiphase Flow, **21**(2), pp. 151–173.
[27] Rukosuyev, M. V., Barannyk, O., Oshkai, P., and Jun, M. B. G., 2016, "Design and Application of Nanoparticle Coating System With Decoupled Spray Generation and Deposition Control," J. Coat. Technol. Res., **13**(5), pp. 769–779.
[28] Lee, J. H., Lee, P., Lee, D., Lee, S. S., and Ko, S. H., 2012, "Large-Scale Synthesis and Characterization of Very Long Silver Nanowires Via Successive Multistep Growth," Cryst. Growth Des., **12**(11), pp. 5598–5605.
[29] Kim, T. Y., Lee, M. J., and Moon, D. G., 2018, "Picosecond Pulsed Laser Irradiation of Silver Nanowire Films Coated on the Polyethylene Terephthalate Substrates," Mol. Cryst. Liq. Cryst., **663**(1), pp. 40–46.
[30] Wipliez, L., Lebrun, L., Kling, R., Fortunier, P., and Fries, L., 2016, "Ultrafast Laser Ablation of Transparent Conductive Silver Nanowire Thin Film on Polyethylene Terephthalate Substrate," J. Laser Appl., **28**(2), p. 022205.
[31] Smits, F. M., 1958, "Measurement of Sheet Resistivities With the Four-Point Probe," Bell Syst. Tech. J., **37**(3), pp. 711–718.